

**Towards a Deeper Understanding of Protein Resistance:
Characterizing Water/Surface and Protein/Surface
Interactions by *In Situ* Neutron Reflectometry**

R. Dahint, M. Skoda, F. Schreiber*, M. Himmelhaus, and M. Grunze*

Applied Physical Chemistry, University of Heidelberg, Germany

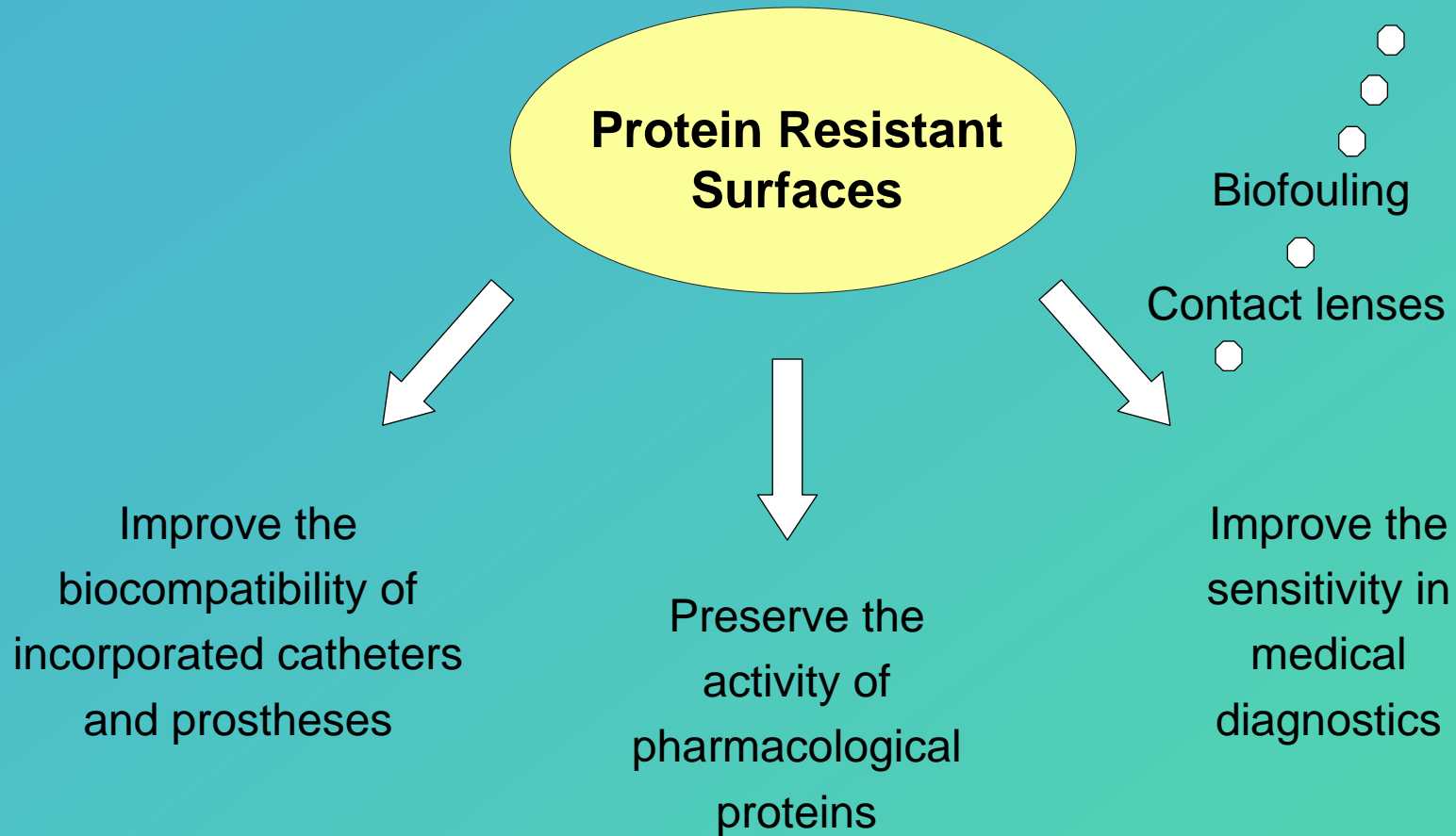
**Institute for Applied Physics, University of Tübingen, Germany*

AVS International Symposium, Boston, Oct. 30 – Nov. 4, 2005

Outline

- Introduction
 - Protein resistant surfaces
 - Oligo(ethylene glycol) (OEG) terminated monolayers
- Proposed models of protein resistance
- OEG/water interfacial structure
- OEG in contact with protein solutions
- Summary and acknowledgements

Protein Resistant Surfaces

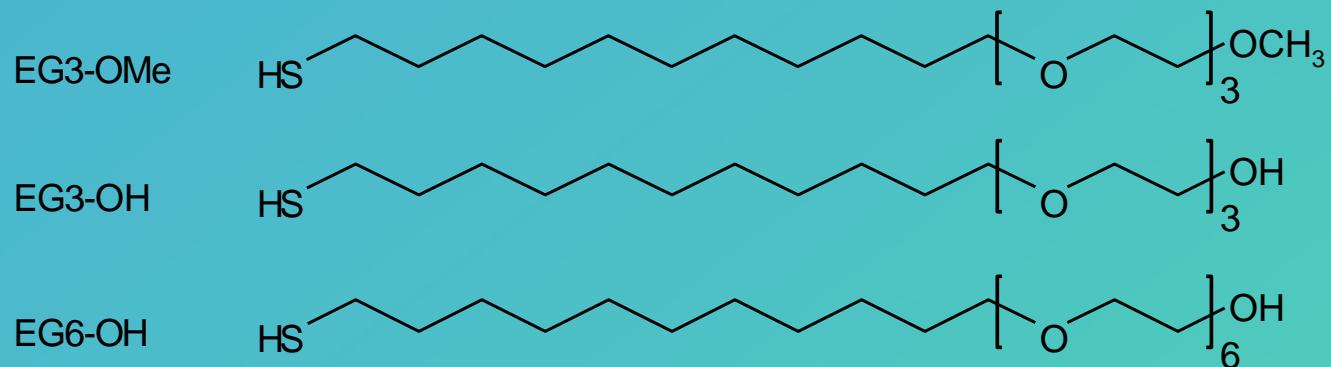


Rational design of protein resistant surfaces

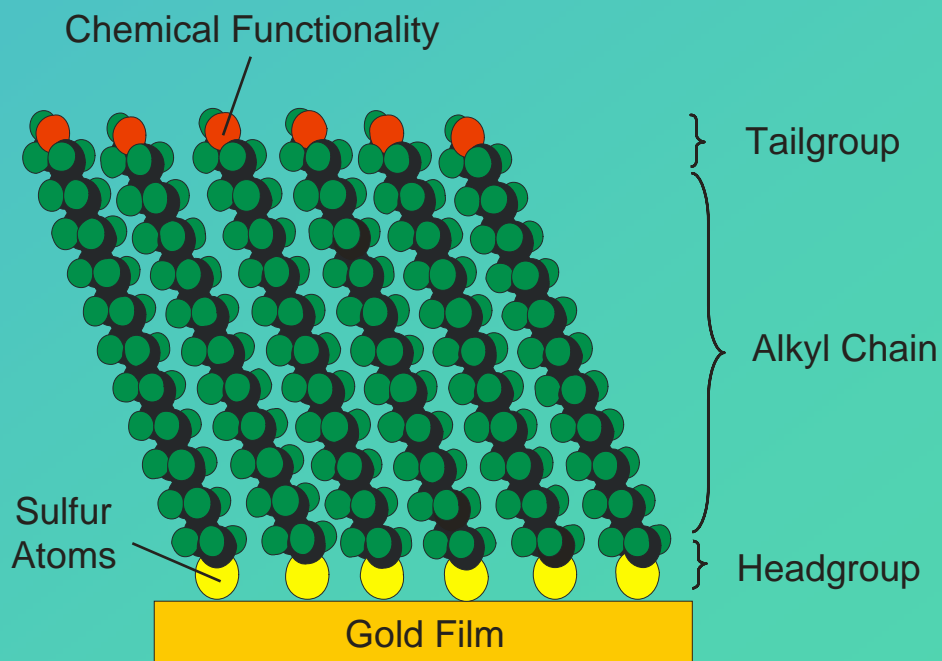


Identification of the relevant physicochemical parameters

Ethylene Glycol (EG) Terminated Alkanethiols: EGn-OR

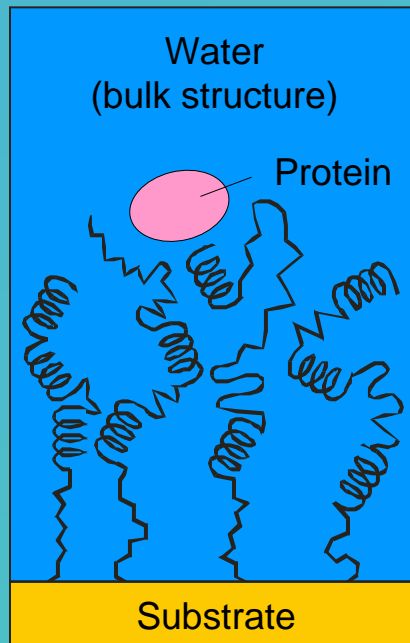


Formation of Self-Assembled Monolayers:



Ethylene Glycol Films: Mechanisms of Protein Repulsion

PEG

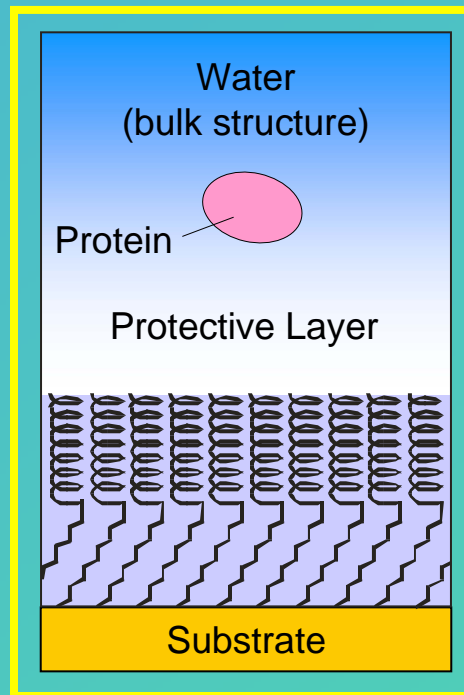


Steric Repulsion

- dehydration
- loss of conformational freedom

Jeon et al., *J. Colloid Interf. Sci.*, 142 (1991) 149

OEG-SAMs

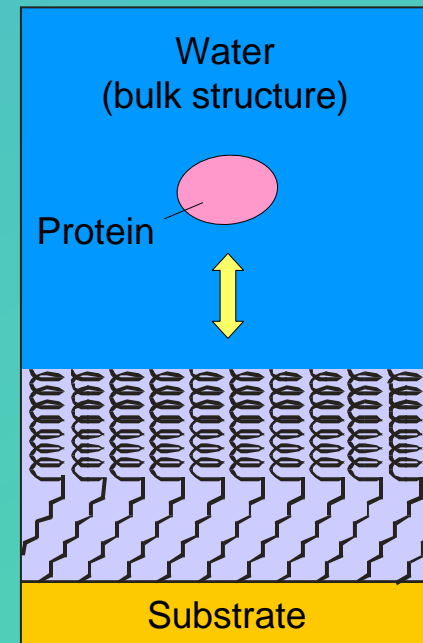


Protective Water Layer?

- firmly bound?
- different structure?

Israelachvili et al., *Nature*, 379 (1996) 219

OEG-SAMs



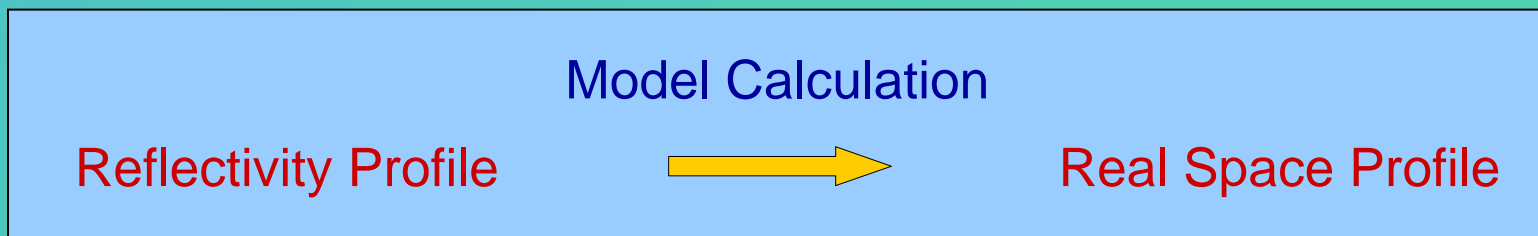
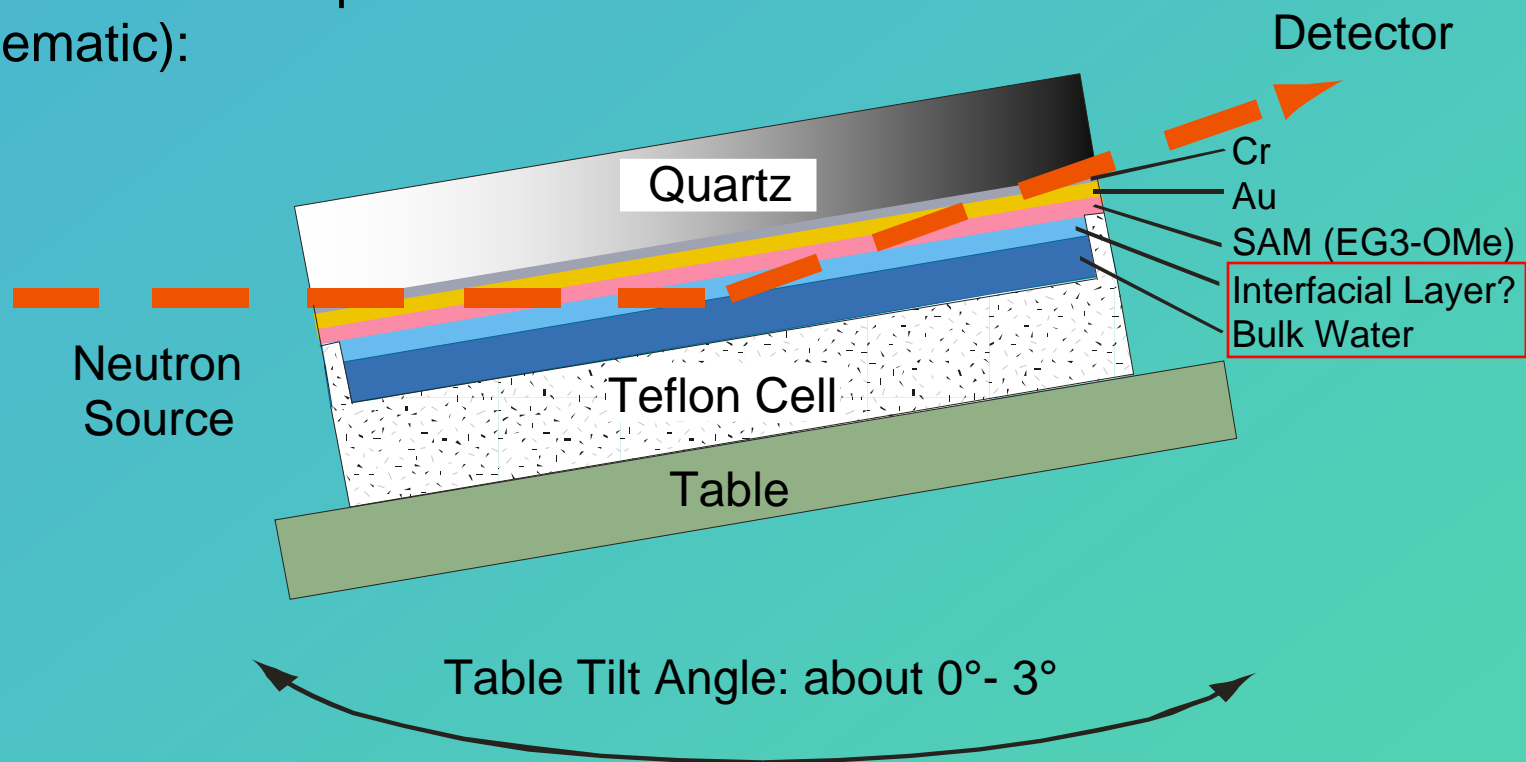
Electrostatic Repulsion?

- exponentially decaying force (measured by AFM)
- scales with Debye length

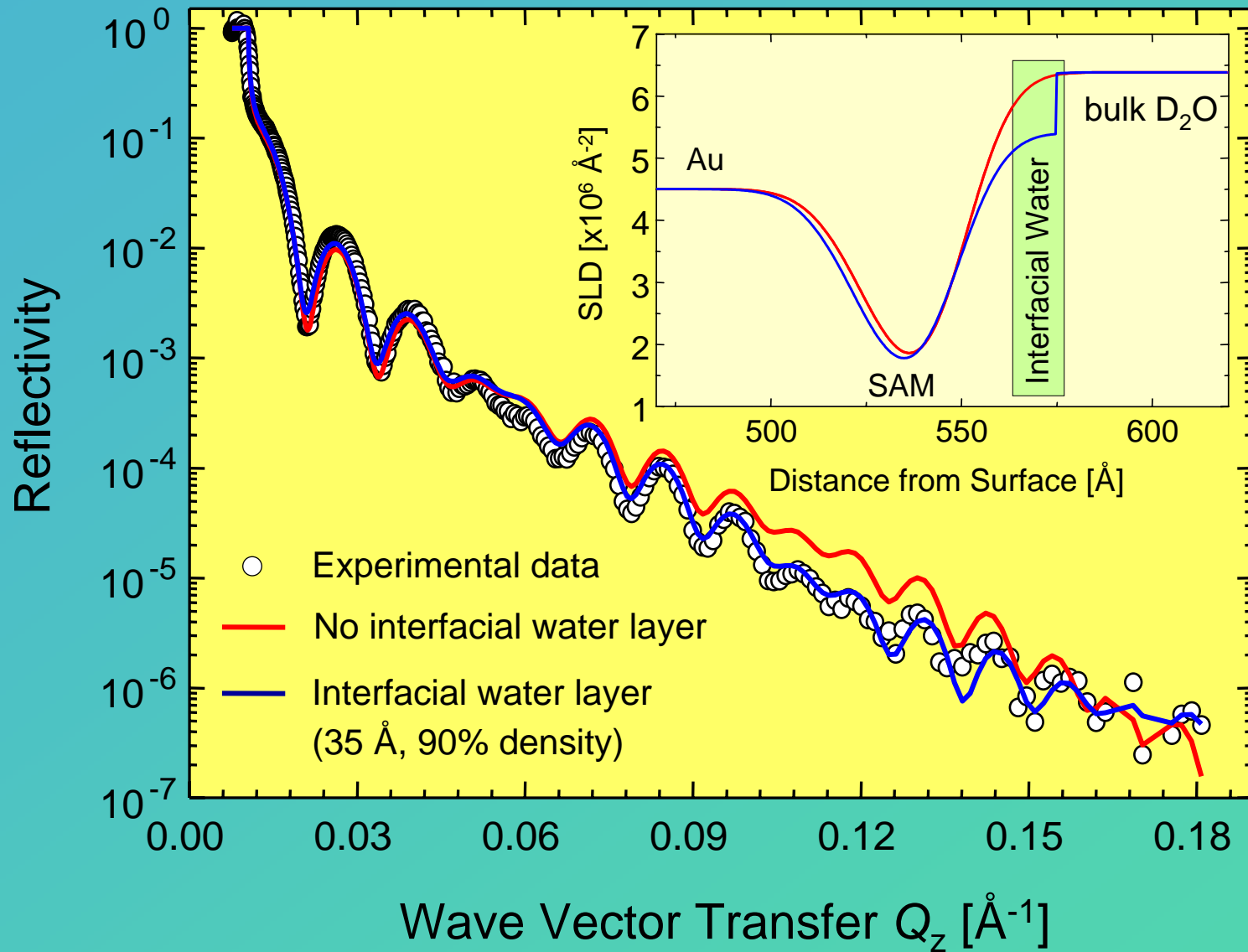
Feldman et al., *JACS*, 121 (1999) 10134

Neutron Reflectometry at SAM/Liquid Interfaces: Schematic

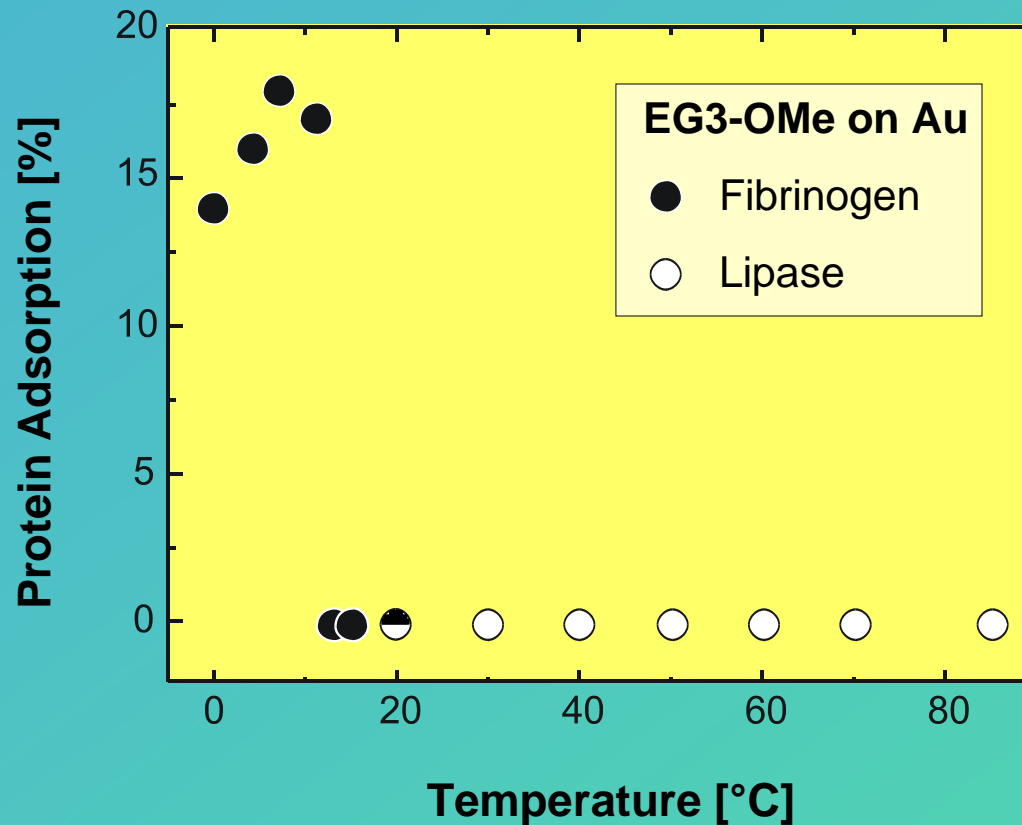
Experimental Setup
(schematic):



Neutron Reflectometry: Interface EG3-OMe/Water



EG3-OMe: Temperature Dependence of Protein Resistance



Protein normalized to fibrinogen adsorption on a hexadecanethiolate SAM on Au at room temperature (about 3.5 ng/mm²)

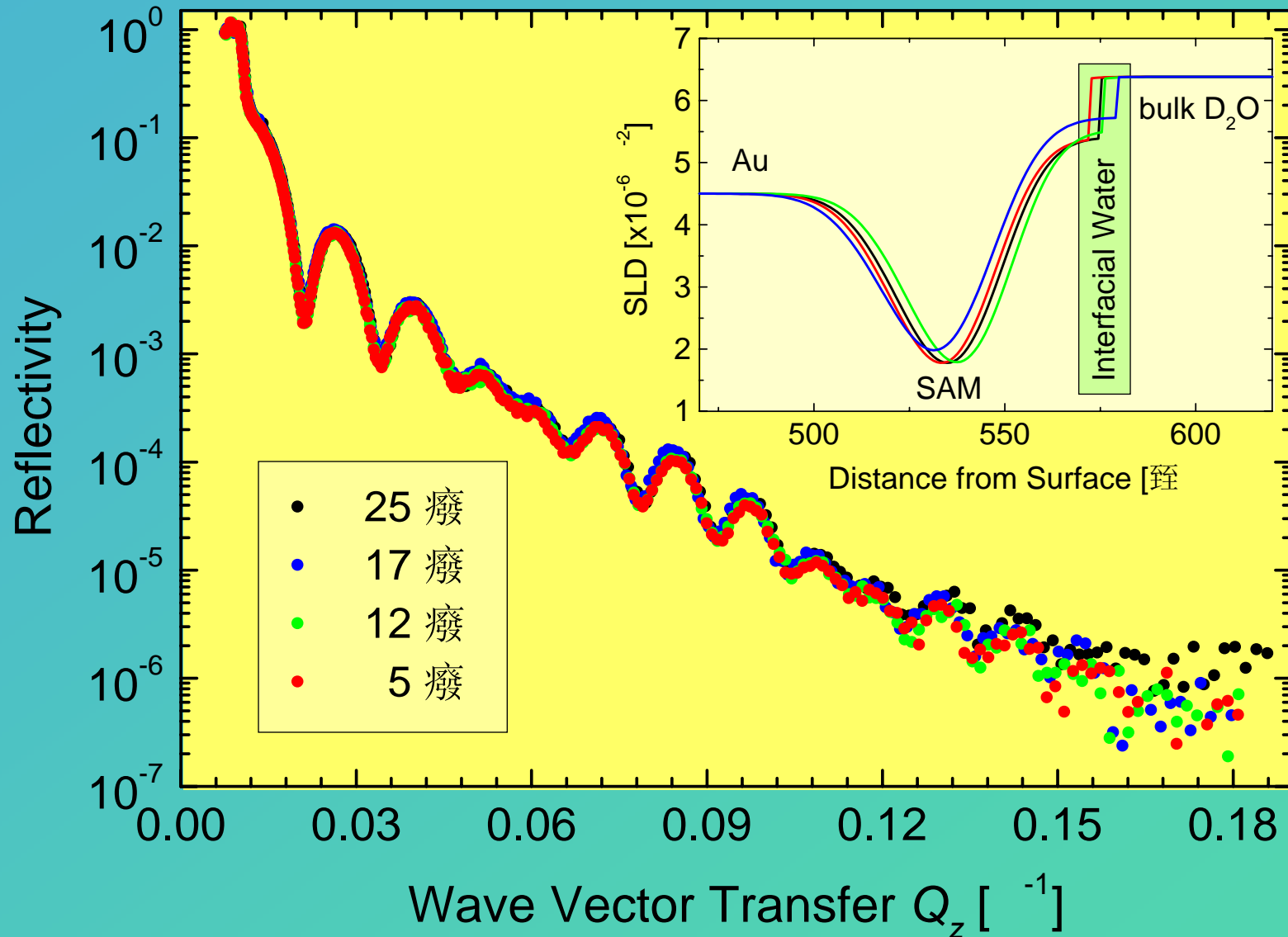
EG3-OMe: Temperature Dependence of Protein Resistance

**EG3-OMe loses its protein resistant properties
below 12°C!**



**Does the interfacial water layer vanish
at low temperatures?**

Interface EG3-OMe/Water: Temperature Dependence



OEG: Interfacial Water Layer and Protein Resistance

**The observed interfacial water layer
does not seem to be
the relevant physicochemical parameter
for rendering OEG surfaces protein resistant!**

Interfacial Water Layer: Effects of Hydrophobicity

EG3-OH and EG6-OH (hydrophilic):

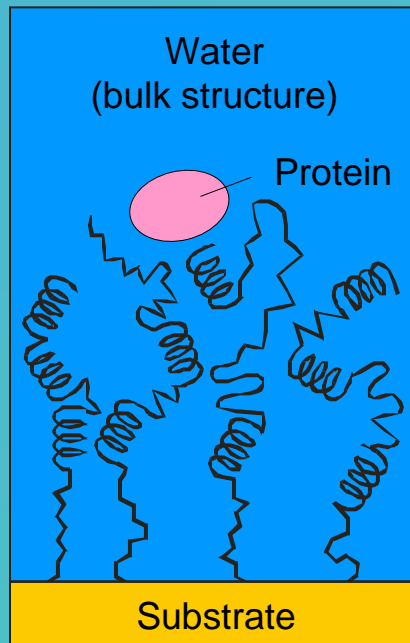
- Protein resistant
- Negligible interfacial water layer

Octadecanethiol, C18 (hydrophobic):

- Protein adsorbing
- Interfacial water layer (2 boxes needed for fitting):
 - 21 Å, 9% of bulk water density
 - 48 Å, 88% of bulk water density

Ethylene Glycol Films: Mechanisms of Protein Repulsion

PEG

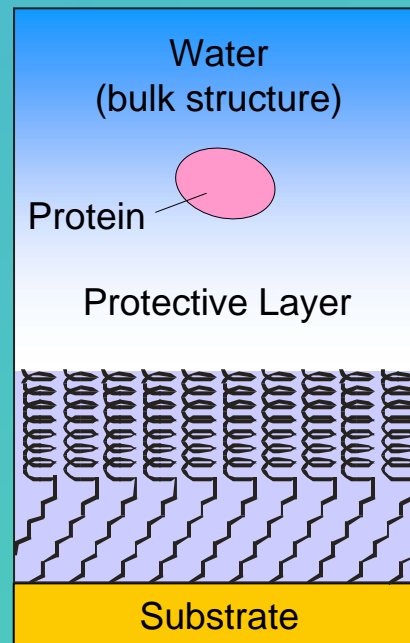


Steric Repulsion

- dehydration
- loss of conformational freedom

Jeon et al., *J. Colloid Interf. Sci.*, 142 (1991) 149

OEG-SAMs

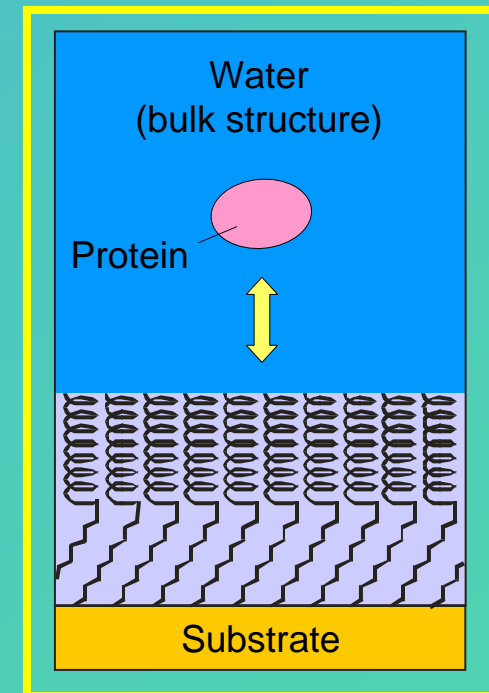


Protective Water Layer?

- firmly bound?
- different structure?

Israelachvili et al., *Nature*, 379 (1996) 219

OEG-SAMs

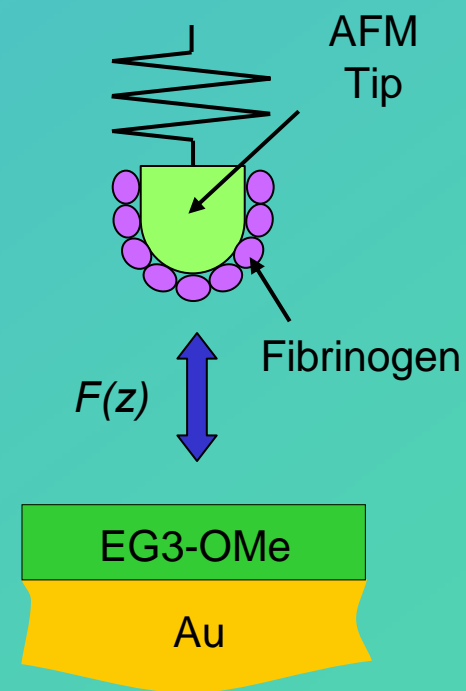
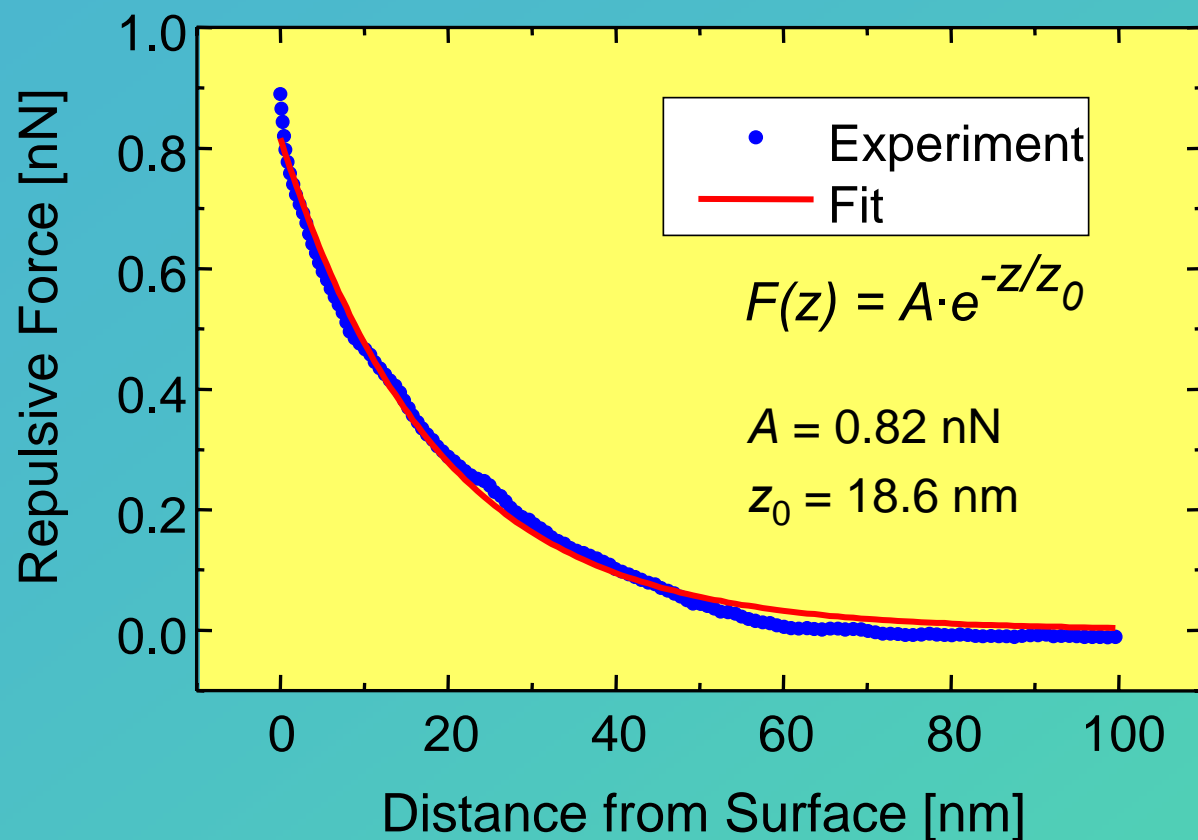


Electrostatic Repulsion?

- exponentially decaying force (measured by AFM)
- scales with Debye length

Feldman et al., *JACS*, 121 (1999) 10134

EG3-OMe: Force/Distance Measurements by AFM



Feldman et al., *JACS*,
121 (1999) 10134

Repulsive force scales with the
Debye length of the solution



Consistent with electrostatic
interactions

Temperature Dependence of Protein Resistance

Adsorbed fibrinogen tends to unfold!



Do native proteins in their natural environment experience the same forces?

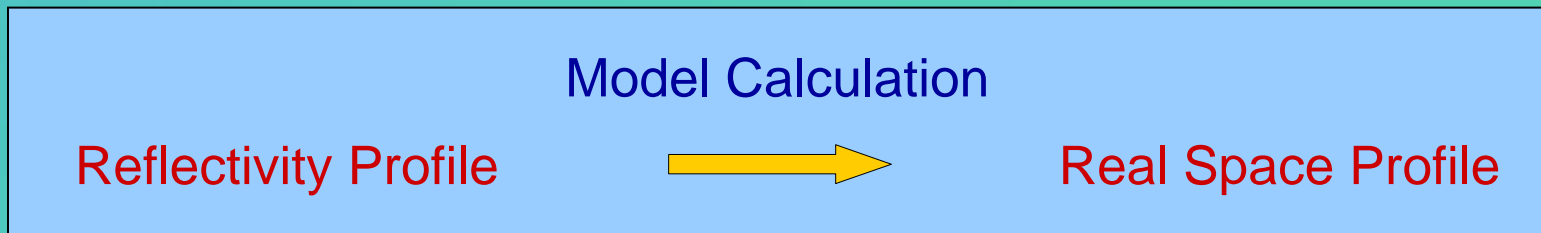
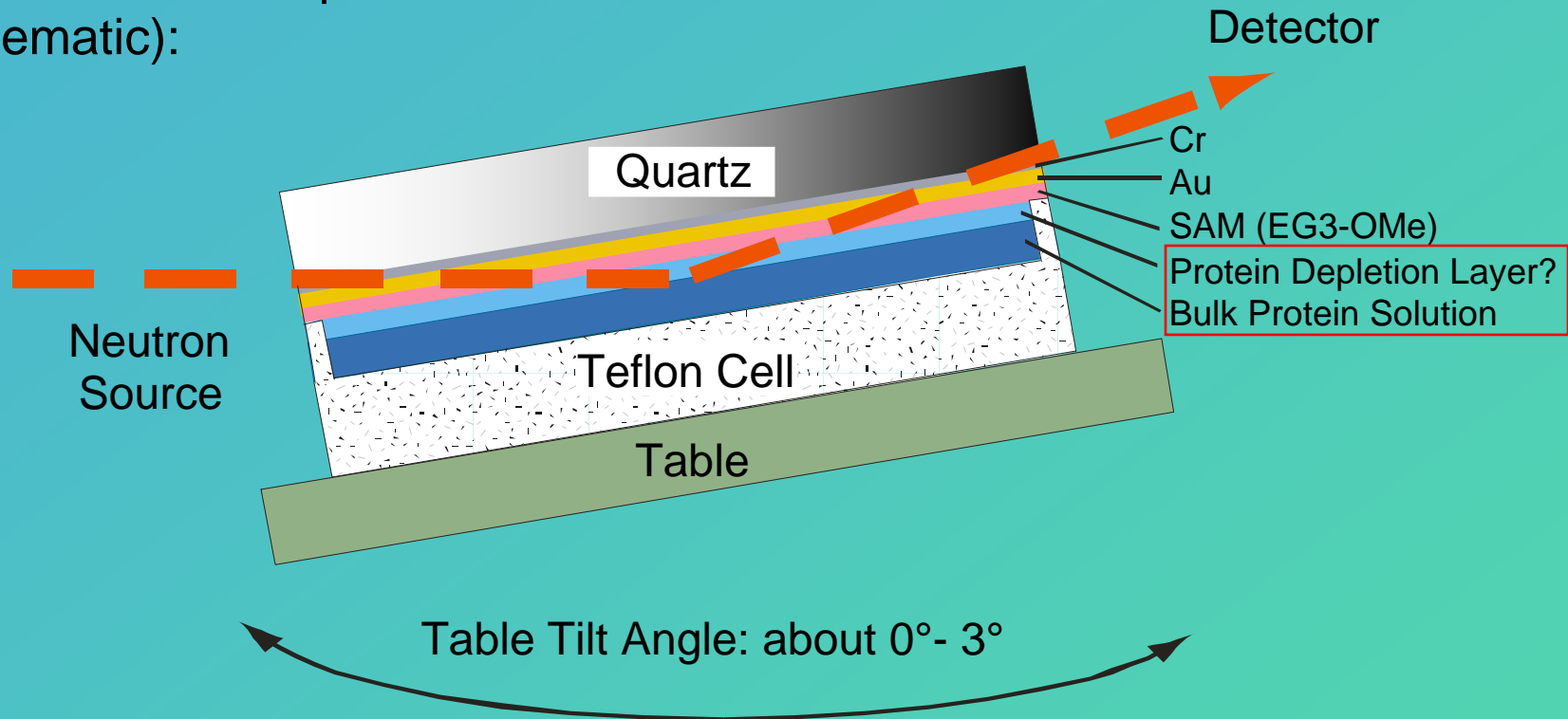


Protein depleted layer in the vicinity of the SAM!

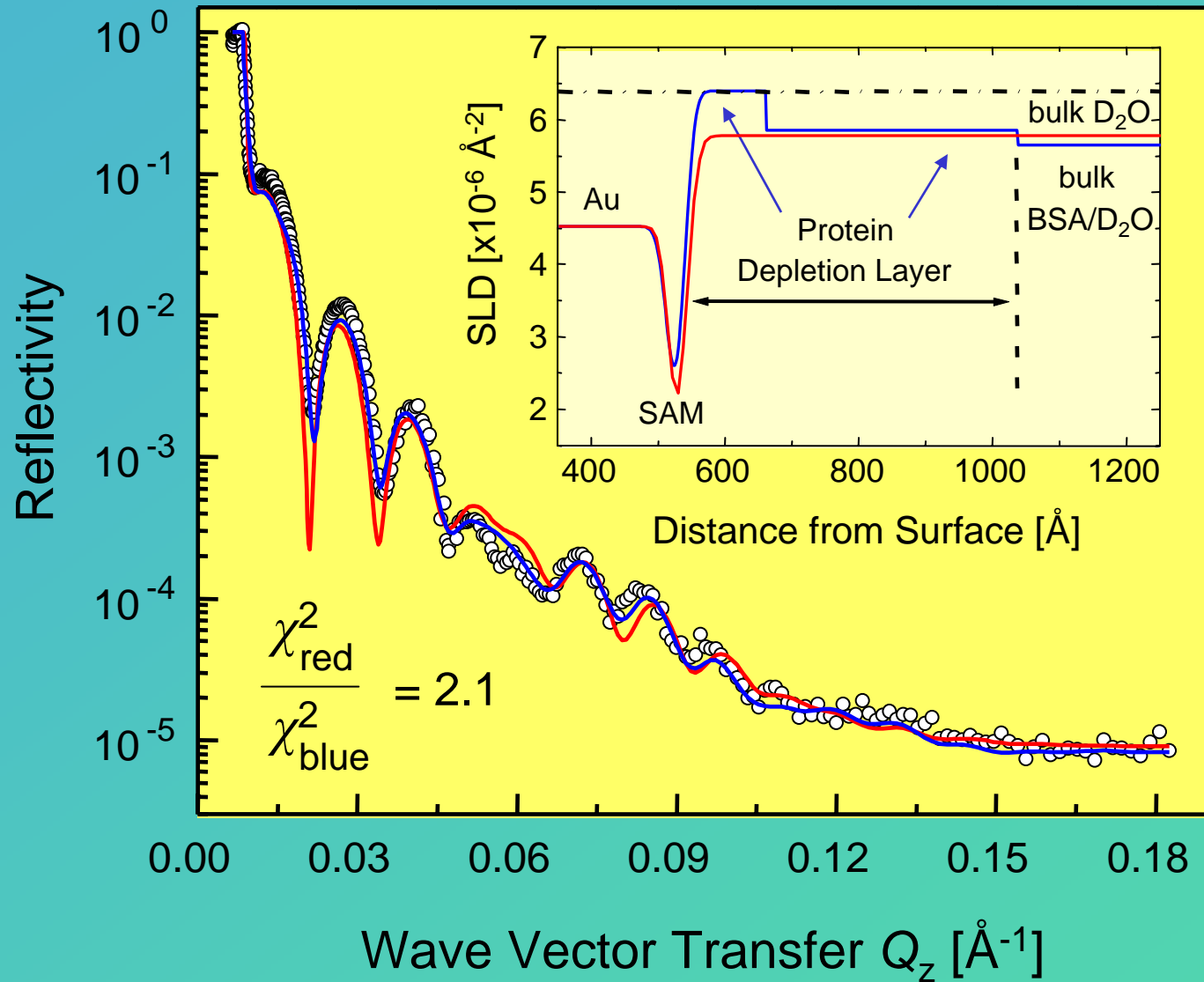
Protein used: Bovine Serum Albumin, BSA (excellent solubility in water)

Neutron Reflectometry at SAM/Liquid Interfaces: Schematic

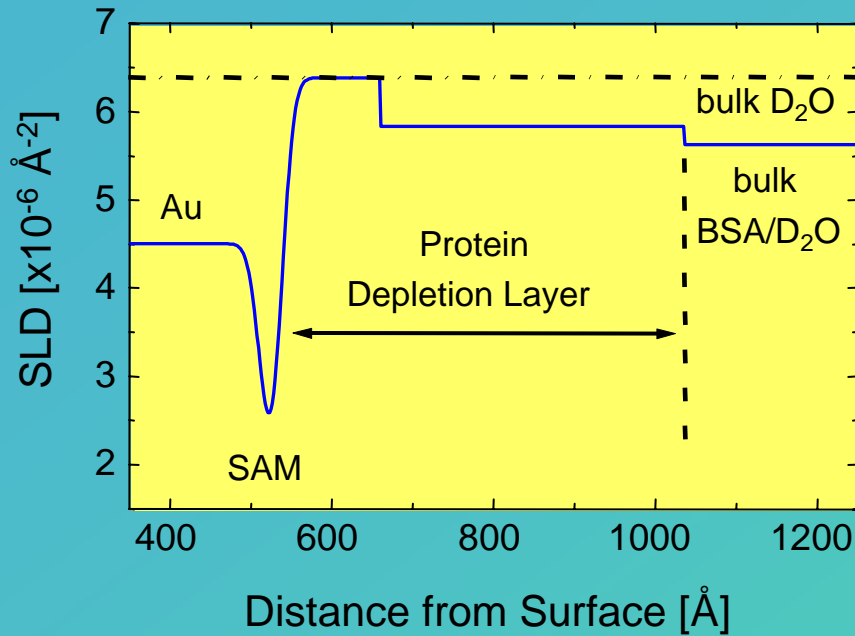
Experimental Setup
(schematic):



EG3-OMe in Contact with Protein Solutions



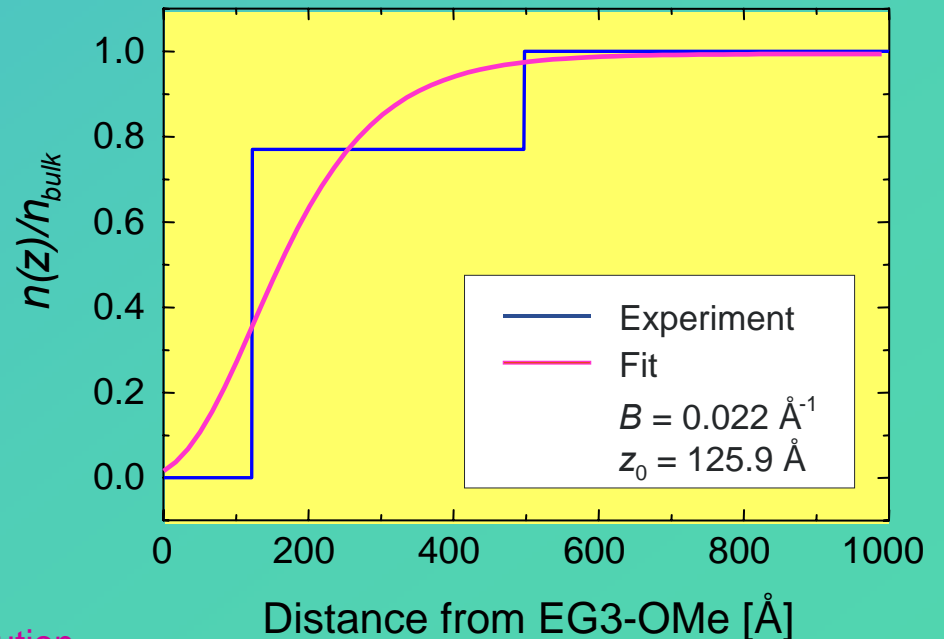
Protein Depletion Layer



Scattering Length Density (SLD)



Protein Concentration Profile



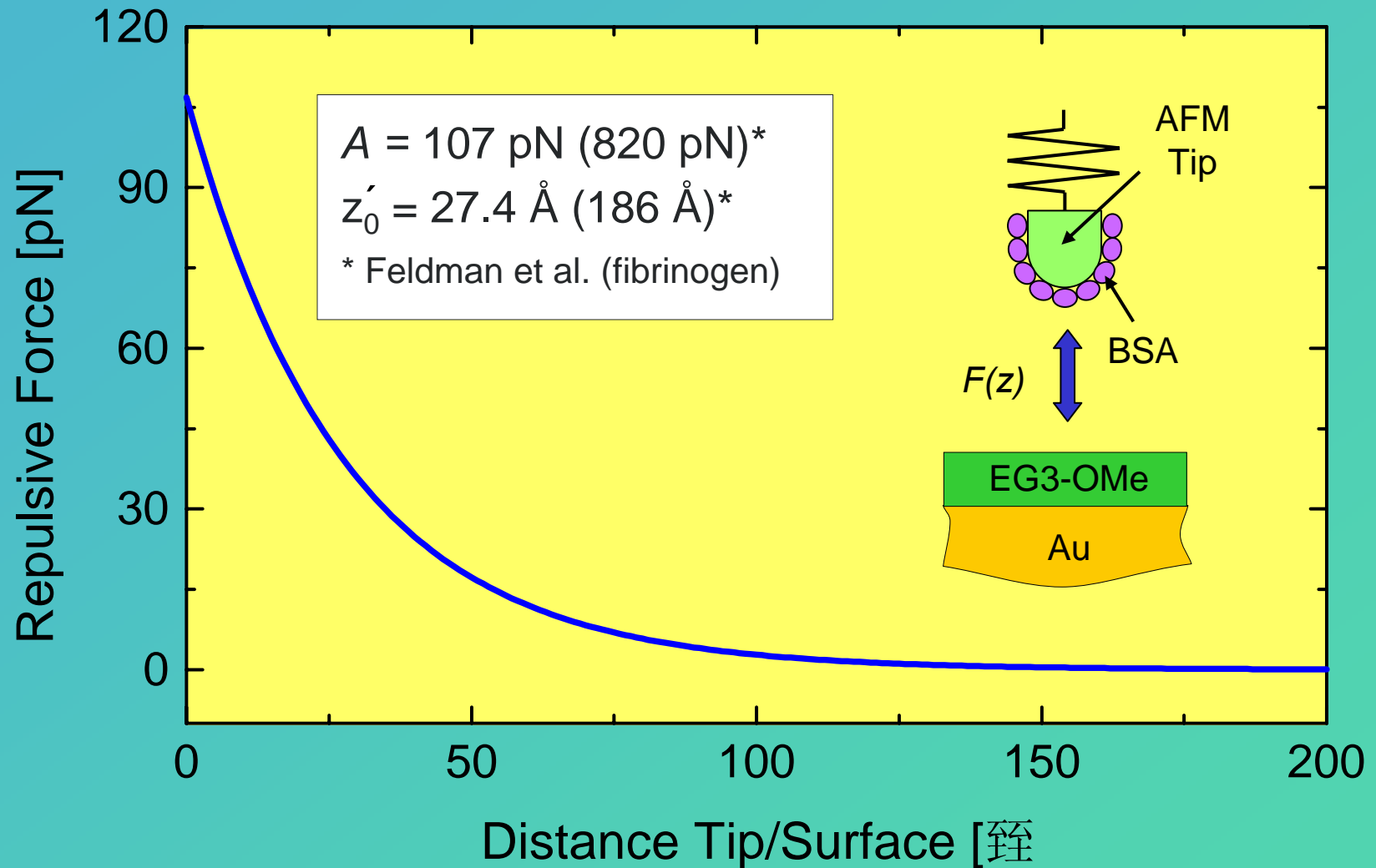
Calculated Protein Concentration Profile:

$$n(z) = n_{bulk} \cdot e^{-z'_0 B e^{-\frac{z-r}{z'_0}}}$$

with $B = \frac{A'}{6\pi\eta rD}$

η : Viscosity, D : Diffusion constant of the protein solution

Calculated Force/Distance Curve for the AFM Experiment



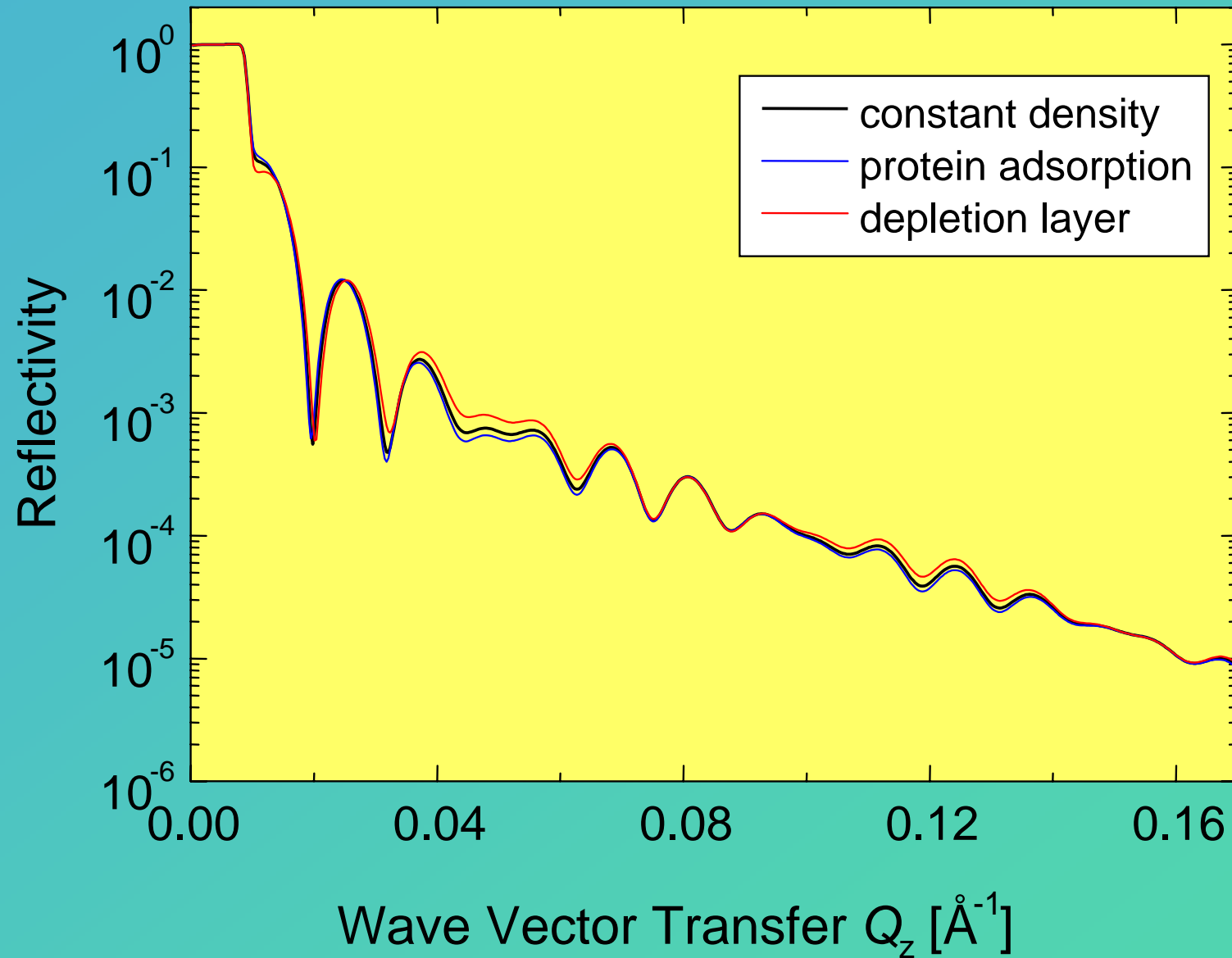
Open Questions

Differences due to

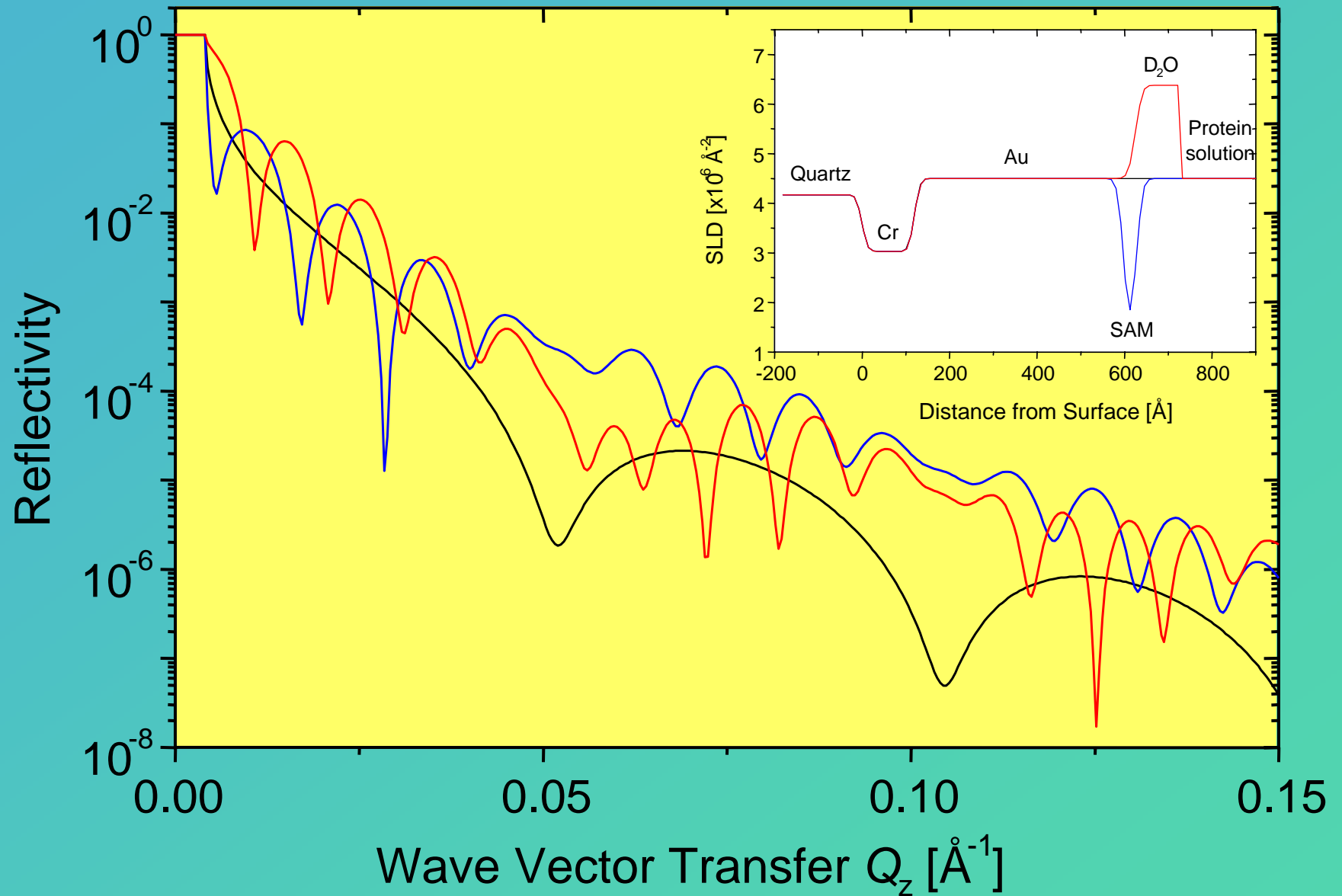
- Different proteins used (BSA vs. fibrinogen)?
- Problems in defining surface contact ($z_0 = 0$) in the AFM measurements?
- Calibration?
- Effects of high protein content (electrolytes of large asymmetry, like proteins, exhibit markedly shorter decay length)?
T. Nylander et al., J. Coll. Interf. Sci., 164 (1994) 136
- Unfolded vs. native proteins?

Needed: Improved sensitivity at the SAM/liquid Interface

Reflectivity Profiles without Contrast Matching



Reflectivity Profiles with Contrast Matching



Summary

- Neutron reflectivity measurements reveal the presence of a density-reduced interfacial water layer in the vicinity of EG3-OMe SAMs
- The protein resistant properties of EG3-OMe cannot be attributed to this interfacial water layer
- In first experiments, the strength and range of protein repulsion has been determined for dissolved molecules in their native environment
- Improved sensitivity to the SAM/liquid interface by contrast matched films

Acknowledgements

Dr. Roland Steitz (V6, Hahn-Meitner-Institute)

Dr. Vincent Leiner (ADAM, ILL)

Dr. Max Wolff (ADAM, ILL)

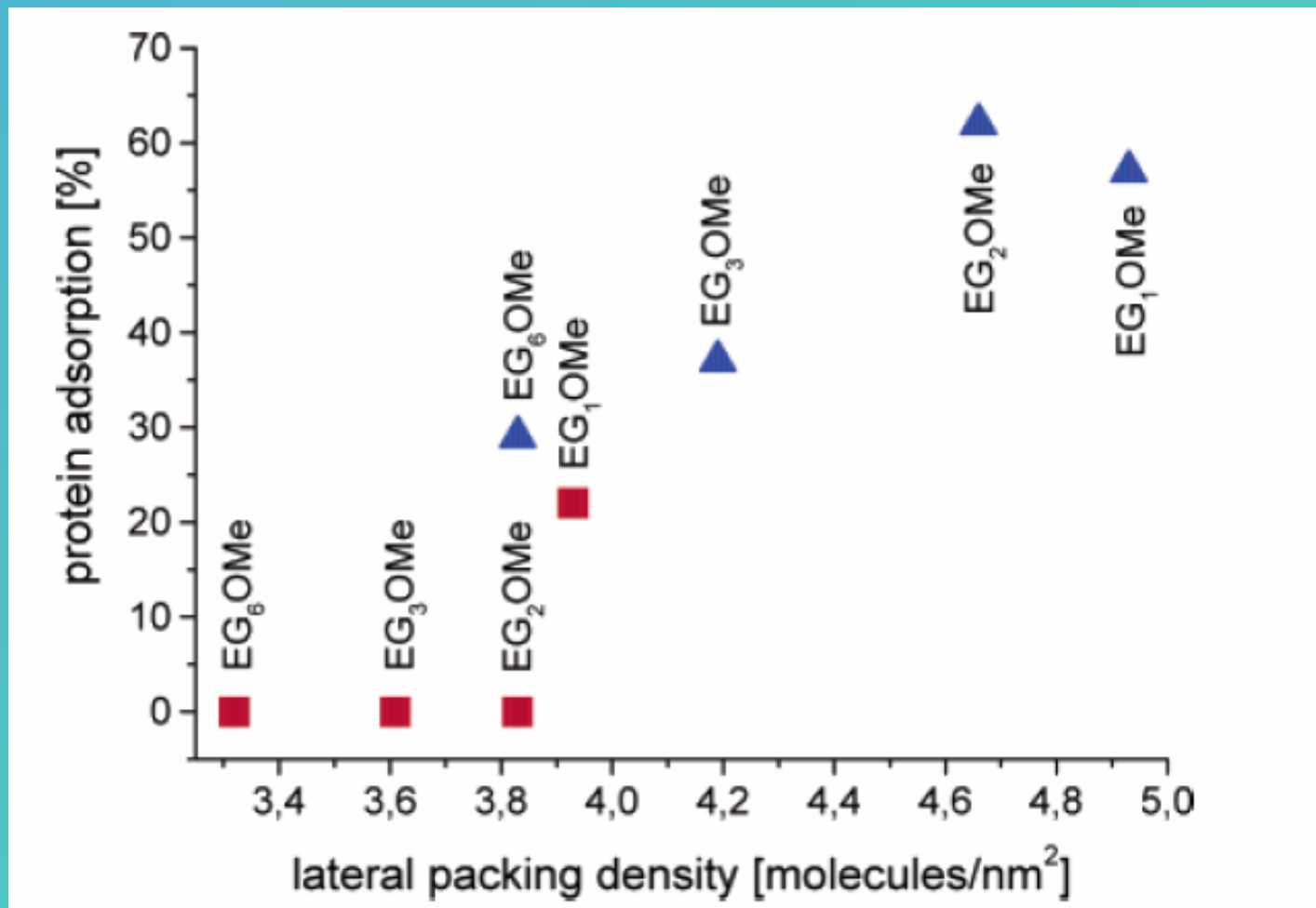
Dr. Robert Cubitt (D17, ILL)

Dr. Jaroslaw Majewski (SPEAR, LANSCE)

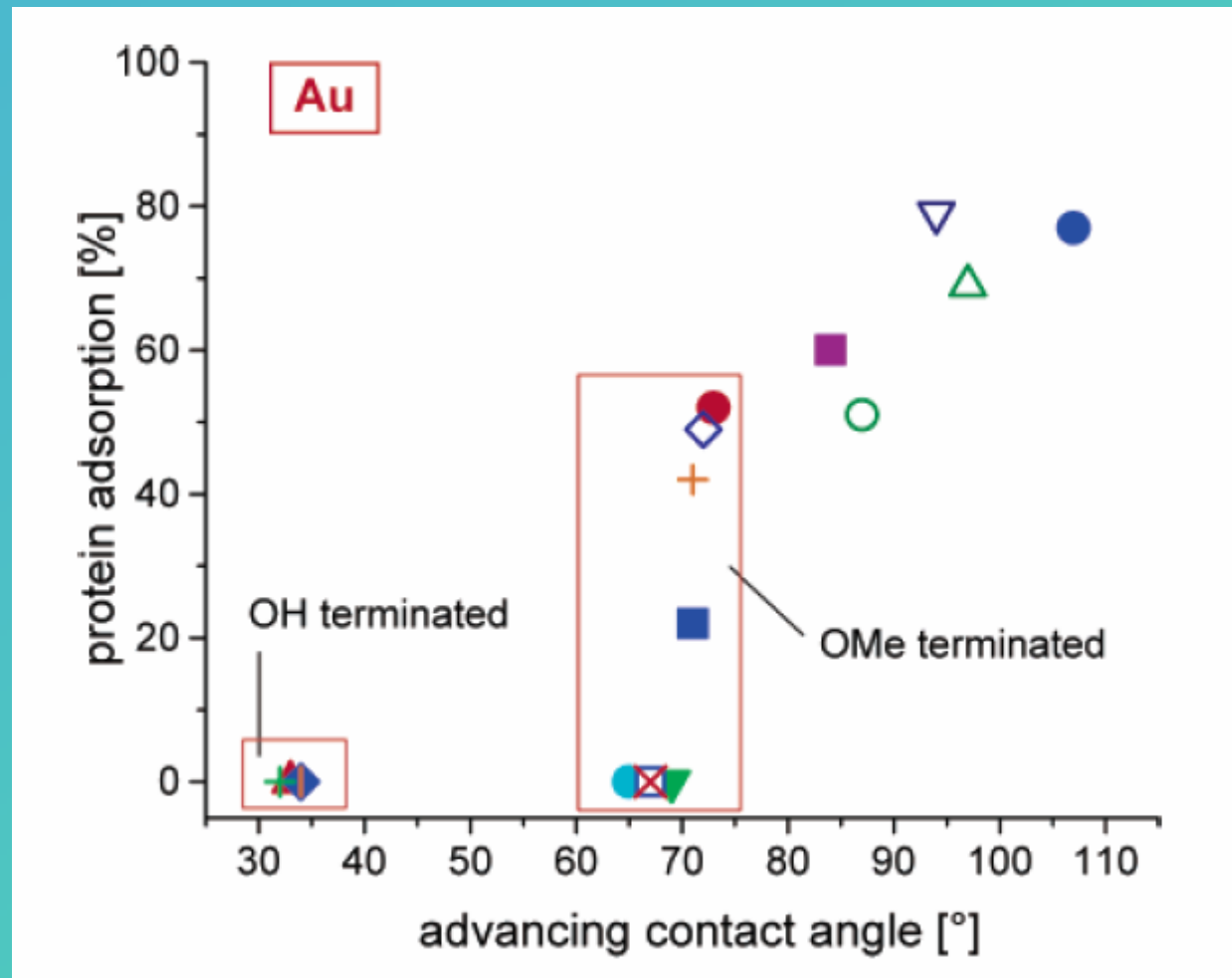
Financial Support:

BMBF, DFG, Max-Buchner-Forschungstiftung, Fond der Chemie

Protein Resistance and Packing Density



Protein Resistance and Hydrophobicity

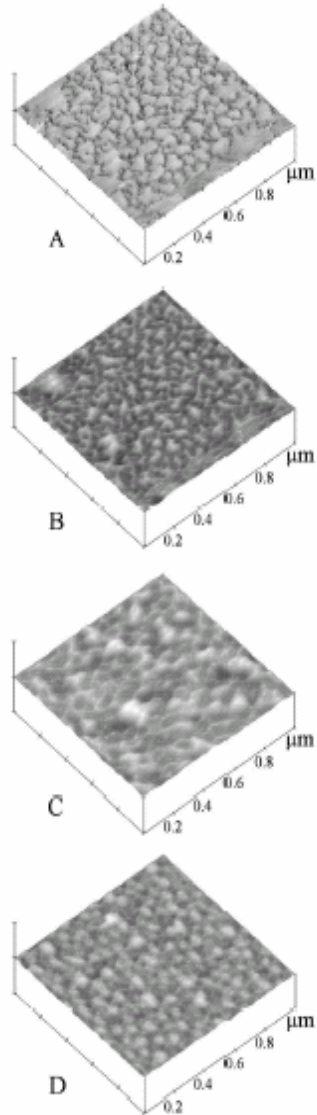


Water in Contact with Hydrophobic Surfaces: Nanobubbles

VOLUME 87, NUMBER 17

PHYSICAL REVIEW LETTERS

22 OCTOBER 2001



of nanobubbles, and that they are, if not contiguous, at least close packed [11]. Analysis of the image shows the individual nanobubbles to have a mean height 20–30 nm, and mean area $4\text{--}6 \times 10^3 \text{ nm}^2$, which increases with decreasing pH. (The area is somewhat dependent on the threshold chosen for the domain decomposition.) At high pH the air-water interface is negatively charged, and the mutual repulsion of the bubbles may account for their more regular shape. No discernable change in morphology or distribution of the bubbles was observed over the several hours of a series of experiments.

Figure 2 shows force curves between the silica colloid and the hydrophobic substrate. The jump into contact seen here arises when the gradient of the attractive force exceeds the cantilever spring constant, and it signifies the bridging of a nanobubble between the two surfaces [1,5]. The separation at which the jump occurs is close to the height of the nanobubbles in Fig. 1. The attraction arises because it is favorable to replace the costly liquid-vapor interface by a solid-vapor interface, and once bridging has occurred the bubble grows laterally. The soft contact or hook region following the jump (inset) has been interpreted as a dynamic effect due to this lateral spreading [5,6]. Calculations predict that the minimum decreases and the width increases with increased driving velocity due to the decreased equilibration time [6], a prediction which the results in Fig. 2 support. Prior to the jump there is a long-range repulsion, as has also been observed previously [5,7]. When artifacts due to laser interference are removed, this repulsion is found to be almost independent of pH and driving velocity and to have a decay length of 25 nm, which is much shorter than the Debye length. The velocity dependence in Fig. 2 also shows that the separation at which the jump occurs decreases with increasing drive velocity. In so far as the jump represents an instability, this is consistent with the notion that a critical fluctuation in the interface is more likely to occur at a larger separation for a slow-moving probe than a fast-moving one because of the longer time it takes to approach.

From the jump-out distance of the retract force in Fig. 2 it is possible to estimate the adhesion as 64–102 nN. This is consistent with a capillary adhesion for a bubble between a flat and a sphere with contact angles of 101° and $80^\circ\text{--}82^\circ$, respectively (calculated in the bridging cylinder approximation [6]). A new feature evident in the retract force following the jump out of contact is the flat, weak attraction and the multiple steps. At large separations bridging bubbles of submicroscopic size are stable with respect to microscopic ones, and conversely at contact, and the attraction due to the former is weak and slowly varying [6]. The data therefore indicate that during the jump out of contact

FIG. 1. AFM tapping mode images of a $1 \mu\text{m}$ square of the hydrophobic glass surface in water. The peak-to-rough scale is 10° in the phase image (A) and 30 nm in the height images (B)–(D). The pH is 5.6 [(A) and the corresponding height image (B)], 3.0 (C), and 9.4 (D).

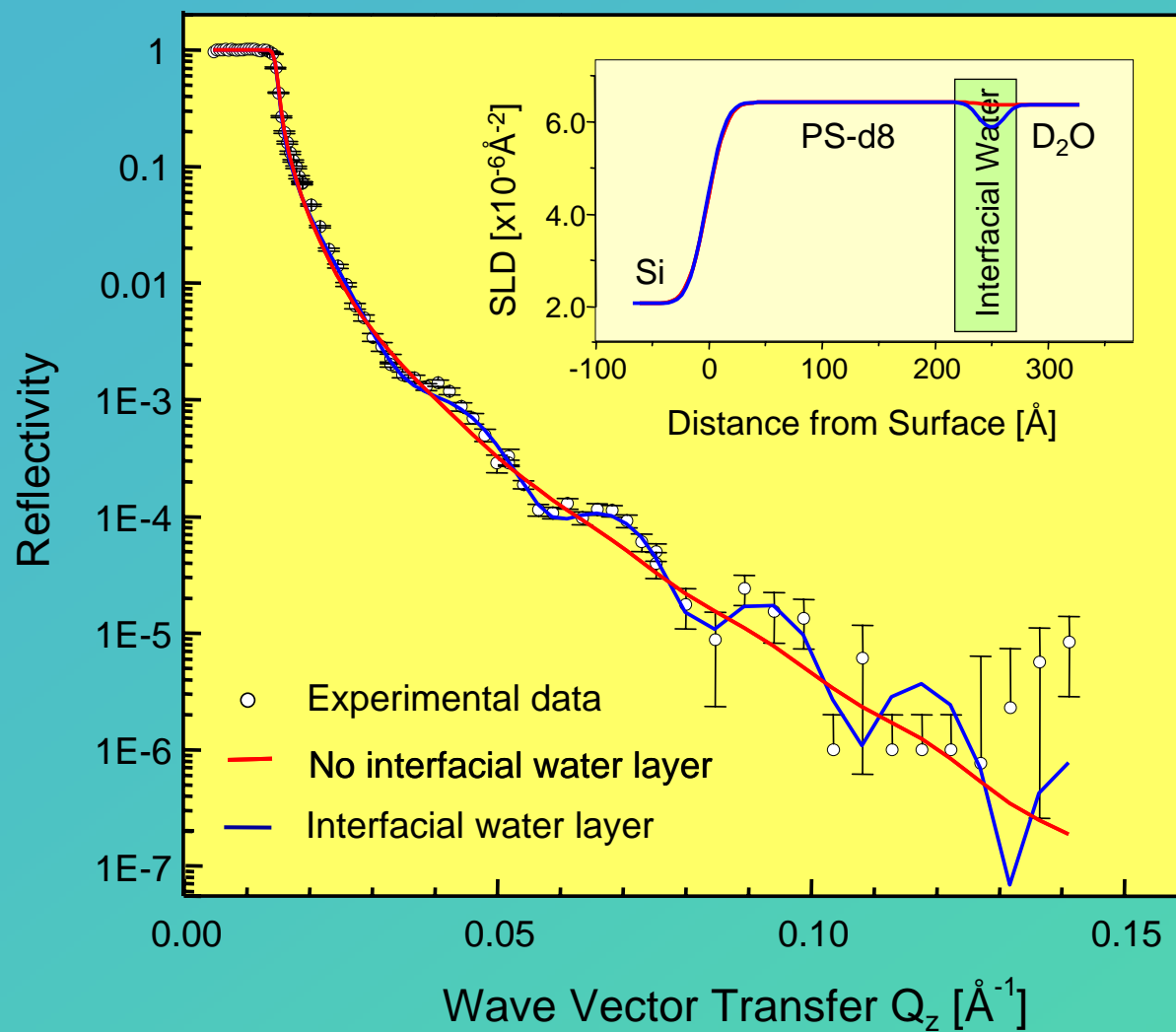
Images of Nanobubbles on Hydrophobic Surfaces and Their Interactions

J.W.G. Tyrrell and P. Attard

Phys. Rev. Lett. 87 (2001) 17

„Imaging of hydrophobic surfaces in water with tapping mode AFM reveals them to be covered with soft domains, apparently nanobubbles that are close packed and irregular in cross section, having a radius of curvature of the order of 100 nm and a height above the substrate of 20-30 nm. . . .“

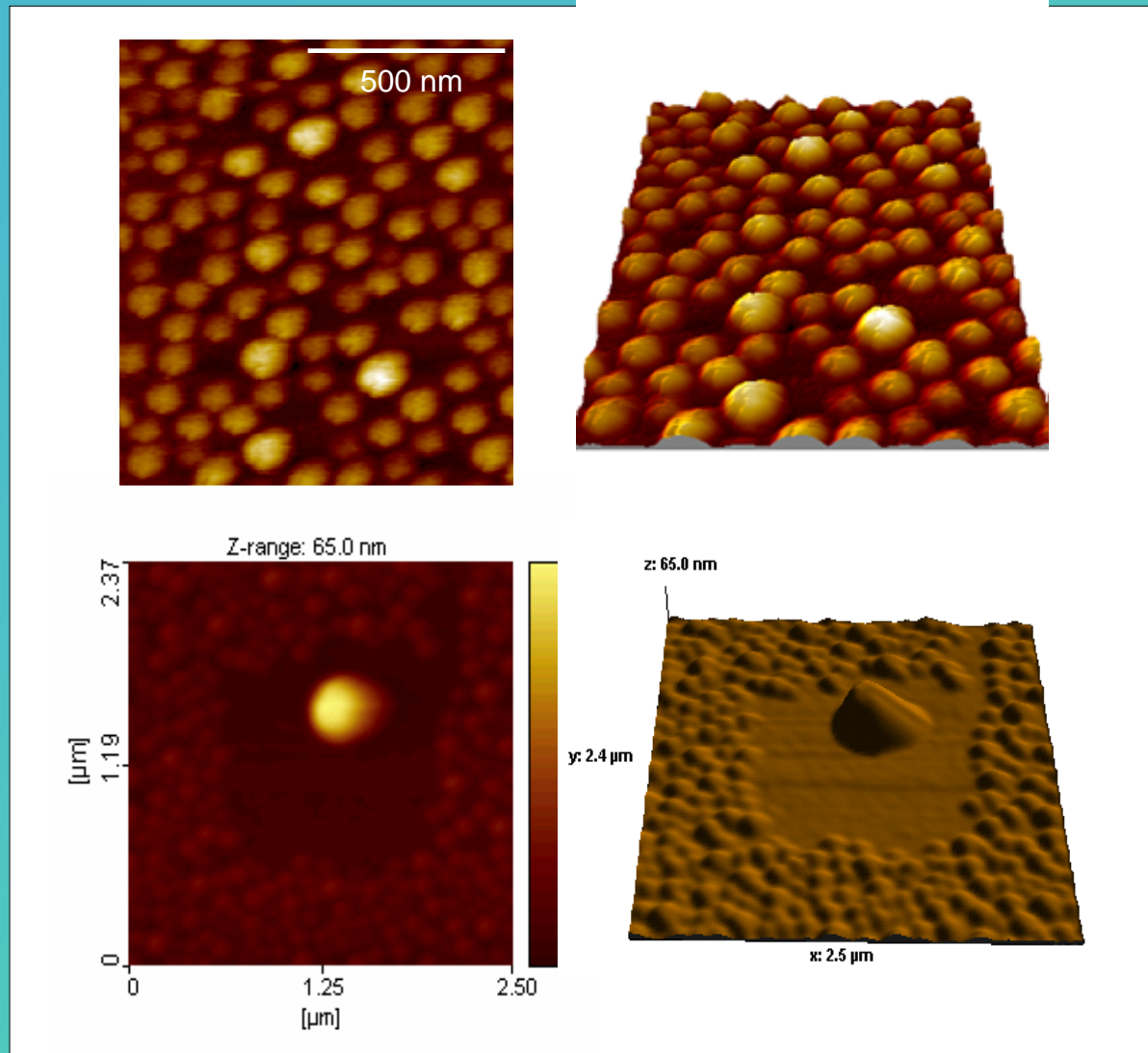
Perdeuterated Polystyrene in Contact with Water



Steitz et al.,
Langmuir,
19 (2003) 2409

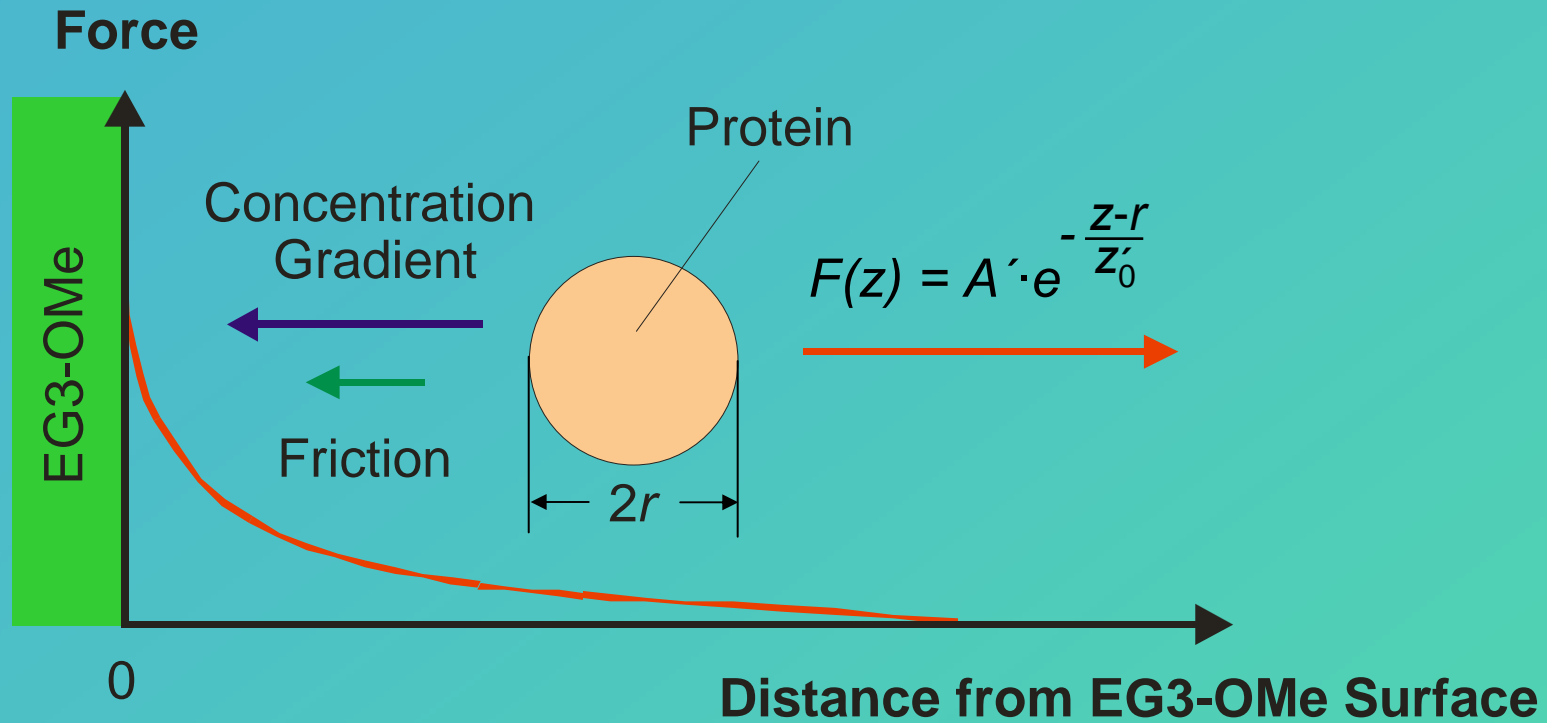
Depletion Layer: 20 – 50 \AA , 88 – 94% bulk D₂O density

Visualization of the d-PS/Water Interface by AFM



Bubble height: 20 nm, radius of curvature ~ 50 nm

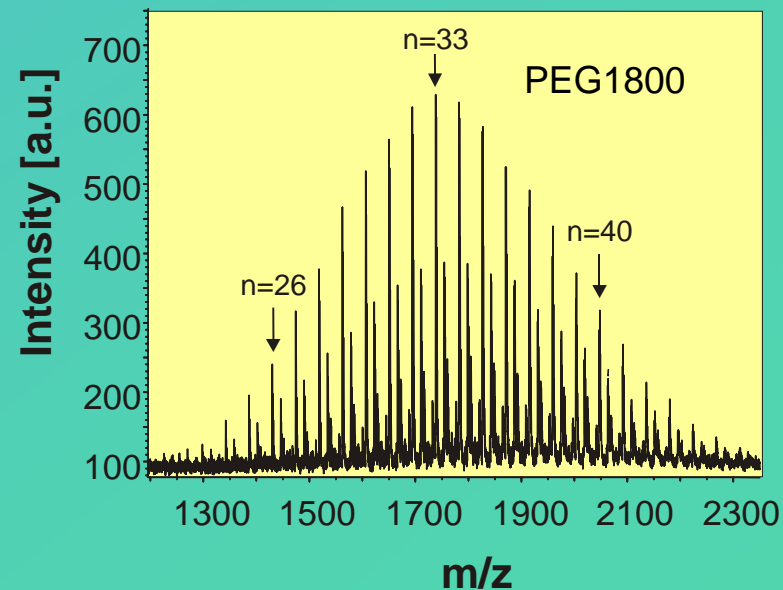
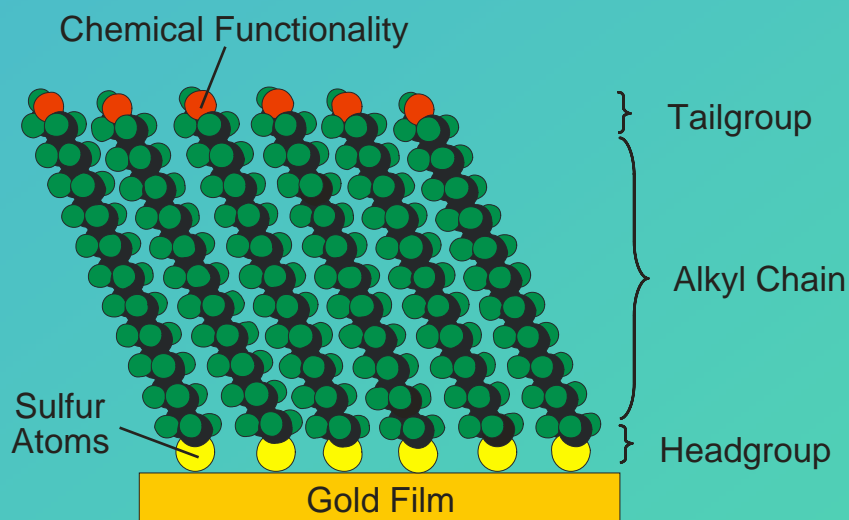
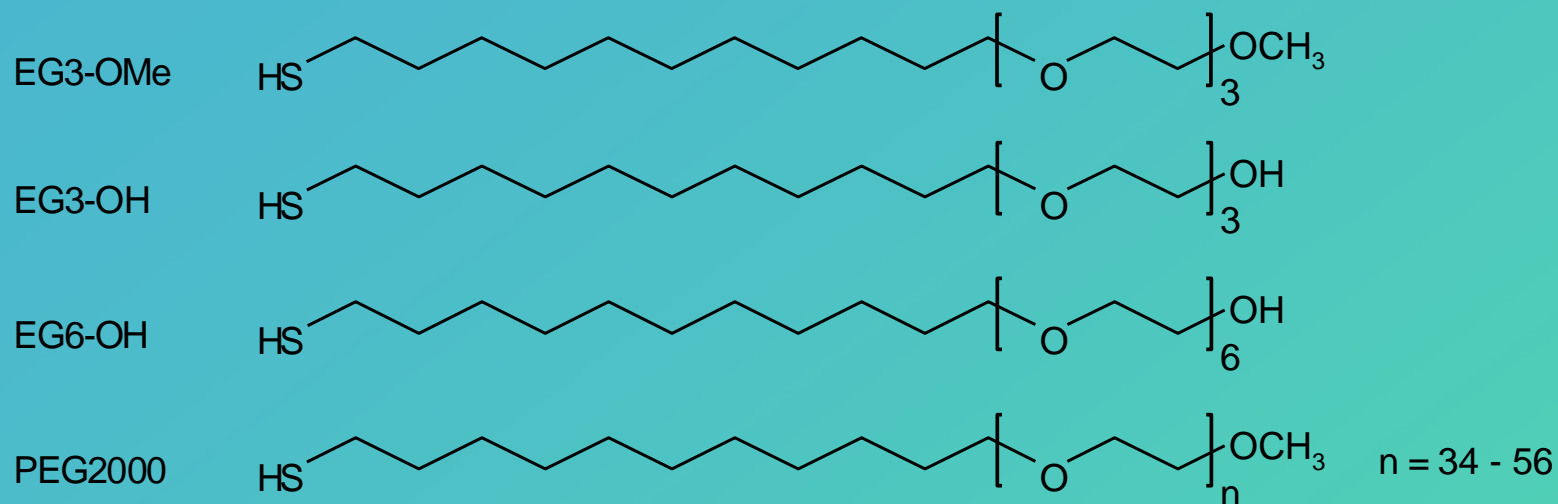
Modeling the Concentration Profile



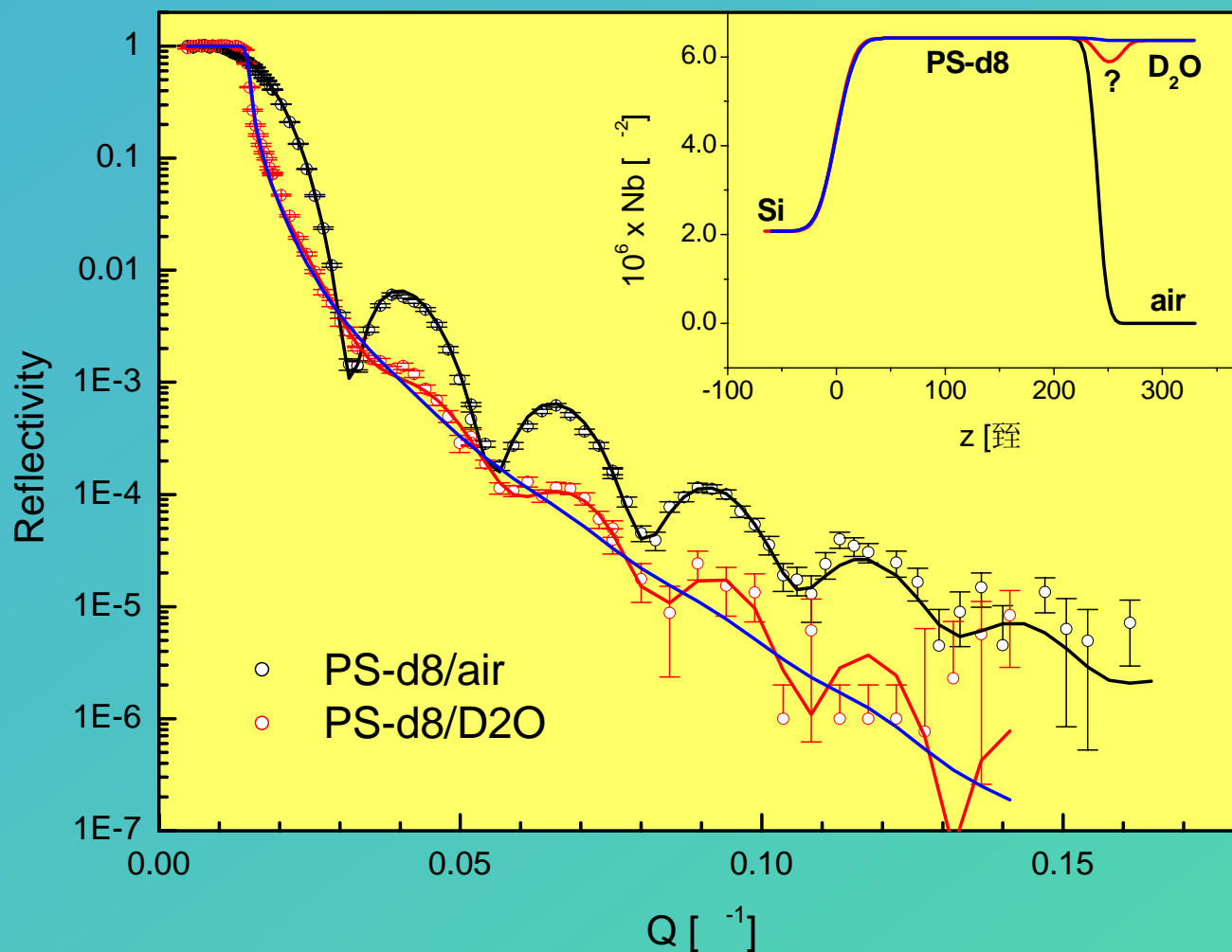
Concentration Profile: $n(z) = n_{bulk} \cdot e^{-z'_0 B e^{-\frac{z-r}{z'_0}}}$ with $B = \frac{A'}{6\pi\eta r D}$

η : Viscosity, D : Diffusion constant of the protein solution

Ethylene Glycol (EG) Terminated Alkanethiols: EG_n-OR



Perdeuterated Polystyrene in Contact with Air and Water



Steitz et al.,
Langmuir,
19 (2003) 2409

Depletion Layer: 20 – 50 Å, 88 – 94% bulk D₂O density